DOI: https://doi.org/10.1063/5.0226934

RESEARCH ARTICLE | OCTOBER 07 2024

Shrimp-shaped structure and period-bubbling route to chaos in a one-dimensional economic model

Special Collection: From Sand to Shrimps: In Honor of Professor Jason A. C. Gallas

Ruma Kumbhakar ; Sarbari Karmakar ; Nikhil Pal ; Jürgen Kurths

Chaos 34, 103115 (2024)
https://doi.org/10.1063/5.0226934

Chaos ARTICLE pubs.aip.org/aip/cha

Shrimp-shaped structure and period-bubbling route to chaos in a one-dimensional economic model

Cite as: Chaos 34, 103115 (2024); doi: 10.1063/5.0226934
Submitted: 5 July 2024 · Accepted: 16 September 2024 ·
Published Online: 7 October 2024

View Online Export Citation CrossMark

Ruma Kumbhakar,[1,a)] Sarbari Karmakar,[1,b)] Nikhil Pal,[1,c)] and Jürgen Kurths[2,3,d)]

AFFILIATIONS

[1]Department of Mathematics, Visva-Bharati, Santiniketan 731235, India
[2]Potsdam Institute for Climate Impact Research (PIK)—Member of the Leibniz Association, Telegrafenberg A56, Potsdam 14473, Germany
[3]Department of Physics, Humboldt University at Berlin, Newtonstraße 15, Berlin 12489, Germany

Note: This paper is part of the Focus Issue, From Sand to Shrimps: In Honor of Professor Jason A. C. Gallas.
[a)]**Electronic mail:** kumbhakarruma@gmail.com
[b)]**Electronic mail:** karmakarsarbari@gmail.com
[c)]**Author to whom correspondence should be addressed:** nikhil.pal@visva-bharati.ac.in
[d)]**Electronic mail:** kurths@pik-potsdam.de and Juergen.Kurths@pik-potsdam.de

ABSTRACT

A beautiful feature of nature is its complexity. The chaos theory has proved useful in a variety of fields, including physics, chemistry, biology, and economics. In the present article, we explore the complex dynamics of a rather simple one-dimensional economic model in a parameter plane. We find several organized zones of "chaos and non-chaos" and different routes to chaos in this model. The study reveals that even this one-dimensional model can generate intriguing shrimp-shaped structures immersed within the chaotic regime of the parameter plane. We also observe shrimp-induced period-bubbling phenomenon, three times self-similarity of shrimp-shaped structures, and a variety of bistable behaviors. The emergence of shrimp-shaped structures in chaotic regimes can enable us to achieve favorable economic scenarios (periodic) from unfavorable ones (chaotic) by adjusting either one or both of the control parameters over broad regions of these structures. Moreover, our results suggest that depending on the parameters and initial conditions, a company may go bankrupt, or its capital may rise or fall in a regular or irregular manner.

The chaos theory has attracted global interest across various fields, including chemistry, physics, materials science, engineering, and economics, to name a few. In this article, the intriguing and captivating dynamical behaviors of a rather simple one-dimensional economic model in a parameter plane are explored with the help of isoperiodic and Lyapunov exponent diagrams. The emergence of shrimp-shaped structures immersed in the chaotic regime and different routes to chaos, namely, period-doubling and period-bubbling routes, are observed. Several types of bistability between various attractors are also found. These insights can aid economists in forecasting possible changes in the financial landscape and making decisions to navigate potential pitfalls effectively. To better visualize the system's dynamics, a few animations are added in the supplementary material.

I. INTRODUCTION

In general, a system is defined as a collection of objects connected in some way, whether physical, biological, social, economic, or any other trait.[1] Systems that follow a consistent set of laws over time are known as dynamical systems. Over the years, the interactions between multiple components of a dynamical system have been elaborated and predicted by formulating mathematical models, usually in two different frameworks, namely, continuous-time dynamical models using differential equations and discrete-time dynamical models using difference equations. Discrete-time dynamical systems are appropriate to model such processes where decisions are repeatedly made over discrete-time intervals. In economics, data are released at discrete intervals, and accordingly, decisions are made. Thus, it is better to formulate an economic system using difference equations in such circumstances where the economic time is discrete due to the inability to revise economic decisions continuously. Aside from this, discrete models have gained tremendous acceptance among researchers for their inherent complex dynamical features over the past few decades in different fields.[2–5] Despite their simplicity and deterministic nature, difference equations are capable of showing a broad range of dynamics, including steady state, periodicity, quasiperiodicity, chaos, etc.[2,3,6,7] In 1974, May[2] studied a one-dimensional discrete-time model considering the logistic growth for a single species population and showed that even such a simple model can exhibit chaotic behavior where it is well known that autonomous nonlinear continuous-time systems cannot exhibit chaos unless it is of dimension at least three. Following May's pioneering work, the chaotic behavior of discrete dynamical systems has been investigated intensively across a variety of disciplines, including physics,[8] ecology,[9] economics,[10] etc. In the context of economics, the chaos theory can well explain the complexity of interactions among consumers, firms, labors, government, financial institutions, and other components of the environment, which lead to the dynamic evolution of industries over time. As a conceptual framework, chaos theory provides a useful way to reconcile industries' inherent long-time unpredictability with their distinctive patterns. The appearance of chaos may be considered undesirable sometimes in economics due to the difficulty in long-term forecasting and unexpected dramatic change, but it is inevitable. Chaos in economics could be used for a wide range of purposes, such as making economic policy, predicting foreign exchange, analyzing stock market movements, or understanding international business dynamics.[11,12] This concept has the potential to play a role in business strategy when it comes to managing complex organizational relationships such as technical collaboration with suppliers and long-term contracts, as well as hybrid forms of organizational control like joint ventures. In addition, chaos helps economic models adapt rapidly to changing conditions, one of the most essential features of the modern world. Hence, from a dynamical point of view, it can be said that the emergence of chaotic behavior in an economic model makes it realistic. For all such reasons, the occurrence of chaos along with other dynamical features of discrete-time economic models, including steady state, periodic, quasiperiodic behaviors, etc., have been extensively explored.[3,13,14] Pohjola[15] discretized Goodwin's growth cycle model[16] along with other modifications and found that the model exhibits chaotic behavior via a period-doubling route. Day[17] modified the Solow model[18] using a difference equation and showed that the system can exhibit periodic as well as chaotic behavior. Bischi and Tramontana[19] applied the concept of the three-dimensional discrete-time Lotka–Volterra model to economics describing the interactions among industrial clusters, and studied the intrinsic dynamics of the system. However, most of these studies regarding the dynamics of an economic system focus on discussing the alterations appearing within the system due to the change of only a single parameter, which is often not sufficient to explore more intricate aspects of the system's behavior. To gain further information of a system's dynamics, a better approach is to analyze the system's behavior by altering at least two parameters simultaneously using tools like isoperiodic diagrams and Lyapunov exponent diagrams. These tools help to uncover complex periodic structures and distinguish among various states within a parameter plane. They are also useful for detecting multistability phenomenon.[20–22] Recently, exploring dynamics of a system in the parameter plane has become popular among researchers, not only in economics[23,24] but also in fields like physics,[5] ecology,[25,26] ecoepidemiology,[27] etc. In the present study, we primarily focus on exploring the complex dynamical behaviors of a one-dimensional discrete-time economic model with the variation of two vital system parameters. In Sec. II, we discuss the construction of the model and present the basic mathematical results. The tangled dynamics of the model are numerically explored in Sec. III using the isoperiodic and Lyapunov exponent diagrams. At last, we end the article with a conclusion.

II. MATHEMATICAL MODEL

Here, we aim to construct a simple one-dimensional discrete-time economic model to capture the change in the company's capital with variations of two system parameters simultaneously. For this, we first consider the following assumptions.

1. Suppose that the growth rate of a company's capital varies with its current capital size, as mathematically represented through the differential equation
$$\frac{dx}{dt} = rx, \tag{1}$$
where x signifies the company's capital and r represents the *per capita* growth rate of capital at any time t. However, the main drawback of system (1) is that it yields exponential capital growth, which contradicts economic realism. It is well known that real-world processes including economic factors like company capital, national income, and labor force, typically exhibit growth saturation due to limited resources. Considering this, we adopt a logistic growth pattern where the company's capital saturates at a certain level. Then system (1) can be modified as
$$\frac{dx}{dt} = rx\left(1 - \frac{x}{k}\right), \tag{2}$$
where k represents the saturation level.
2. It is essential to note that a minimum capital threshold is required for a company to function profitably. If the invested capital falls below this threshold, the company suffers losses and eventually faces bankruptcy. This is incorporated as follows:
$$\frac{dx}{dt} = rx\left(1 - \frac{x}{k}\right)\left(\frac{x}{A} - 1\right), \tag{3}$$
where A denotes the threshold value, which lies between 0 and k.
3. It can also be assumed that the company invests a portion of the capital in some other companies, or some other companies and organizations invest a portion of funds in the company, i.e., there is always an outflow or inflow of a portion of the capital. Incorporating this notion, system (3) can be written as
$$\frac{dx}{dt} = rx\left(1 - \frac{x}{k}\right)\left(\frac{x}{A} - 1\right) - f(x), \tag{4}$$
where $f(x)$ signifies the rate of capital outflow or inflow.

It is well known that economic decisions cannot be revised continuously, rather those are taken at discrete-time intervals. Therefore, it is more appropriate to modify system (4) using a discrete-time framework. Now, considering $f(x) = \alpha x$, i.e., a linear outflow or inflow of the capital and using the forward Euler algorithm with step-size 1, system (4) can be written in a discrete-time setup as

$$x_{n+1} = x_n + r x_n \left(1 - \frac{x_n}{k}\right)\left(\frac{x_n}{A} - 1\right) - \alpha x_n, \tag{5}$$

where x_n represents the company's capital at the *nth* time period. The parameters r, k, and A are taken to be positive for economic significance. α represents the *per capita* outflow or inflow rate of the capital and can take both positive and negative values based on outflow or inflow of capital.

Before exploring the intrinsic dynamical behaviors of system (5) with extensive numerical simulations, first, we briefly present the existence and stability criteria of its fixed points along with the bifurcations occurring around them in Subsection II A.

A. Mathematical results

The fixed points of system (5) can be determined by solving

$$g(x) = x, \tag{6}$$

where $g(x) = x + rx\left(1 - \frac{x}{k}\right)\left(\frac{x}{A} - 1\right) - \alpha x$.

We see that system (5) has three fixed points, namely, the trivial fixed point and a pair of non-zero fixed points. Here, we briefly discuss the existence criteria along with the stability criteria of these fixed points.

First, let us denote $\beta_1 = (k-A)^2 - \frac{4\alpha A k}{r}$, $\beta_2 = r\left(\frac{A}{k} + \frac{k}{A}\right)$, and $\beta_3 = r\left(\frac{1}{k} + \frac{1}{A}\right)$.

Now, it is analytically found that

- the trivial fixed point $E_0 = 0$ always exists and is stable if $0 < r + \alpha < 2$;
- the non-zero fixed point $E_1 = \frac{(k+A) + \sqrt{\beta_1}}{2}$ exists if $\beta_1 > 0$ and is stable if $0 < 2 + r + 2\alpha - \frac{\beta_2}{2} - \frac{\sqrt{\beta_1}\beta_3}{2} < 2$; and
- the non-zero fixed point $E_2 = \frac{(k+A) - \sqrt{\beta_1}}{2}$ exists if $\beta_1 > 0$ and is stable if $0 < 2 + r + 2\alpha - \frac{\beta_2}{2} + \frac{\sqrt{\beta_1}\beta_3}{2} < 2$.

Remark II.1. *For $\beta_1 = 0$, there exists only one non-zero fixed point $E^* = E_1 = E_2 = \frac{k+A}{2}$ (with multiplicity 2). At this point, $g'(E^*) = 1$ and $g''(E^*) = -r\left(\frac{1}{A} + \frac{1}{k}\right)$. Hence, E^* is semi-stable.*

Bifurcations

Now, we analytically determine the bifurcations occurring within system (5) due to the variation of the parameter α.

First, let us denote $M = \sqrt{(k-A)^2 - \frac{4\alpha_1 A k}{r}}$, where α_1 lies on the curve $2 + r + 2\alpha - \frac{\beta_2}{2} - \frac{\sqrt{\beta_1}\beta_3}{2} = 0$, and $N = \sqrt{(k-A)^2 - \frac{4\alpha_2 A k}{r}}$, where α_2 lies on the curve $2 + r + 2\alpha - \frac{\beta_2}{2} + \frac{\sqrt{\beta_1}\beta_3}{2} = 0$ with $\beta_1 > 0$.

We find that system (5) undergoes

- a flip bifurcation around E_0, if $\alpha + r = 2$ and $\frac{\beta_3^2}{r} \neq \frac{1}{kA}$;
- a transcritical bifurcation around E_0, if $\alpha + r = 0$;
- a flip bifurcation around E_1, if $(k + A + M)\left(\beta_3 + \frac{3rM}{Ak}\right) \neq 4$ and $\left(\beta_3 + \frac{3rM}{Ak}\right)^2 \neq \frac{4r}{Ak}$;
- a saddle-node bifurcation around E_1, if $r + 2\alpha - \frac{\beta_2}{2} - \frac{\sqrt{\beta_1}\beta_3}{2} = 0$ where $\beta_1 > 0$; and
- a flip bifurcation around E_2, if $(k + A - N)\left(\beta_3 - \frac{3rN}{Ak}\right) \neq 4$ and $\left(\beta_3 - \frac{3rN}{Ak}\right)^2 \neq \frac{4r}{Ak}$.

To visualize the stability of the fixed points and bifurcations around them, we present a diagram in the $r - \alpha$ parameter plane following the existence and stability criteria of the fixed points, where k and A are fixed at 1 and 0.7, respectively (see Fig. 1). In Fig. 1, the entire $r - \alpha$ parameter plane is divided into eight different regions, each distinguished by a distinct color. The system's dynamics in these colored regions are described on the right side of Fig. 1. The system exhibits bistability in the regions R_2, and R_6. It is interesting to note that the system undergoes flip bifurcations along the Flip curves, transcritical bifurcations along the TB curve, and saddle-node bifurcations along the SN curve.

III. NUMERICAL SIMULATIONS

In this section, we perform numerical simulations of system (5) with the aid of MATLAB to shed more light on the intricate dynamics inherent in the system. Here, each diagram results from running the simulations for a total of 10^5 iteration steps and the first 5×10^4 iteration steps are discarded to eliminate transient effects. We also fix the values of the parameters k and A at 1 and 0.7, respectively, and the initial state at $x_0 = 0.3$ throughout the simulations unless we specify it.

First, we draw two bifurcation diagrams together with Lyapunov exponent (LE) diagrams for the variation of the two vital control parameters r and α [*per capita* rate of outflow ($\alpha > 0$) or inflow ($\alpha < 0$) of the capital] separately in order to study the evolution of system (5). In Fig. 2, we draw the bifurcation diagram [Fig. 2(a)] and its associated LE diagram [Fig. 2(b)] by varying the parameter r. From both diagrams, it is clear that as the parameter r increases, system (5) gradually enters into a chaotic state around the fixed point E_1 via a period-doubling route. When $r < 0.2297$, the system remains stable. However, at the critical value $r = 0.2297$, a flip bifurcation occurs, leading to periodic behavior. Further increase in r results in a series of period-doubling bifurcations, leading to chaotic oscillations (around E_1) and this persists up to $r = 1.483$. However, for $r > 1.483$, the system becomes stable

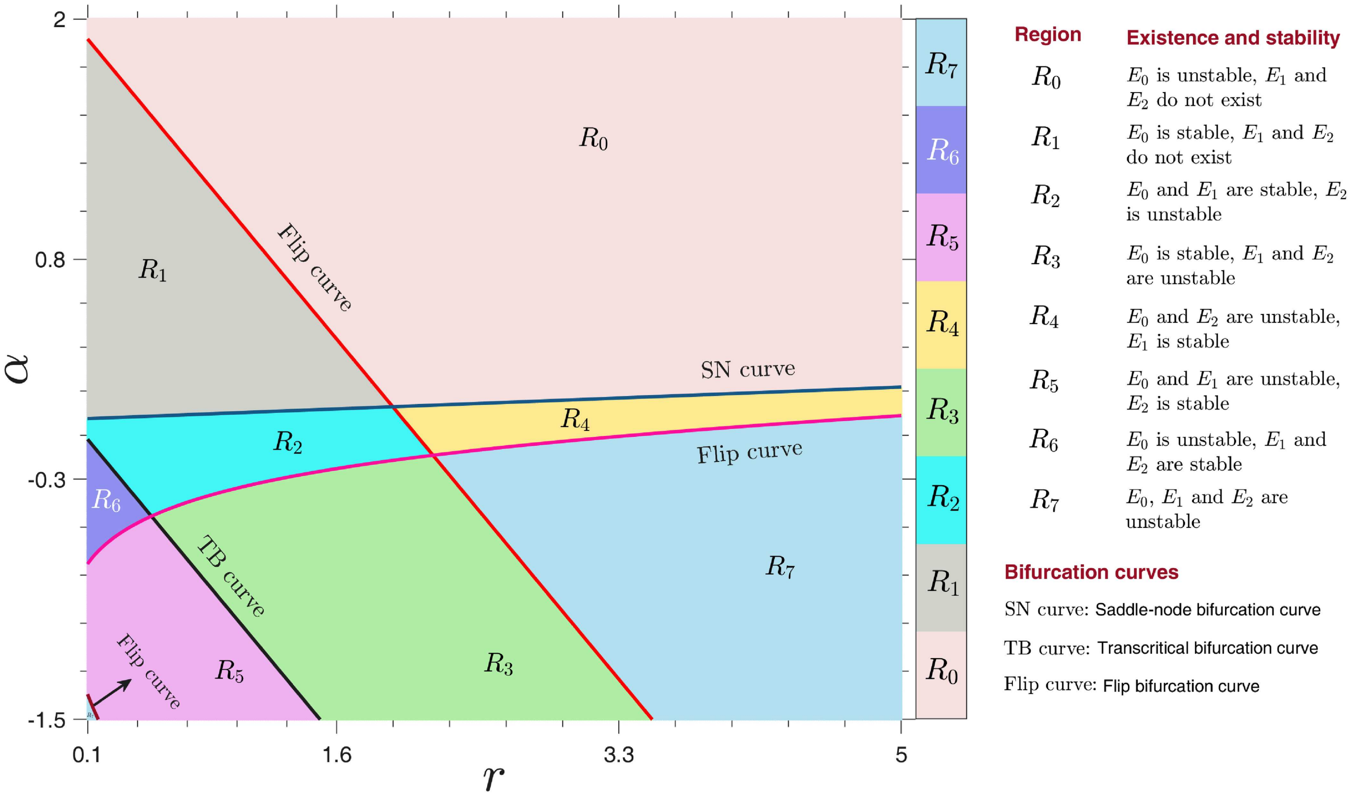

FIG. 1. Regions of different dynamical scenarios present in the $(r, \alpha) \in [0.1, 5] \times [-1.5, 2]$ parameter plane of system (5). Here, $k = 1$ and $A = 0.7$.

around the fixed point E_0. As r increases further, the system becomes periodic via a flip bifurcation (around the fixed point E_0) at $r = 2.61$ and eventually becomes chaotic around the fixed point E_0 through a series of period-doubling bifurcations.

To observe the dynamical behaviors of the system for the changes of the parameter α, we now draw the bifurcation diagram [Fig. 3(a)] and the associated LE diagram [Fig. 3(b)] for the variation of the parameter α within the range $[-1.1, 0.6]$. We see that the system becomes periodic via a flip bifurcation (around the fixed point E_0) from the stable state as α crosses the threshold value -0.9. As α increases further, a series of period-doubling bifurcations takes place, and the system becomes chaotic around the fixed point E_0.

To put it briefly, system (5) exhibits complex dynamical behaviors that are significantly influenced by the parameters r and α. Moreover, there are some clearly visible periodic windows inside the chaotic zones of both diagrams. For a more immersive depiction of the evolving dynamical scenarios brought about by changes in the control parameters r and α, we have included two animations, "Anim_bif_r.mp4" and "Anim_bif_ α.mp4," in the supplementary material. Now, the individual variation of these control parameters (r and α) provides only partial insights of the behavior of the system. However, it fails to give its complete overview. To overcome this limitation, it is essential to systematically study the impact of simultaneous variation of these two parameters (r and α) on system (5). Through this two-parameter analysis, it is also possible to study the organization of the periodic structures embedded within the chaotic regimes and characterize the regimes of multistability formed by overlappings among different attractors. This serves as a focal point of interest in this article. First, we will analyze the two-dimensional isoperiodic diagram of system (5) in the $r - \alpha$ parameter plane, and its iterative zooms to uncover finer intricate behaviors. We will also examine the underlying LE diagram of the associated isoperiodic diagram within the same selective region of the $r - \alpha$ parameter plane.

Figures 4(a) and 4(b) are the isoperiodic and LE diagrams of the system (5) in the $(r, \alpha) \in [0.1, 5] \times [-1.5, 2]$ parameter plane, respectively. Each diagram is set up on a dense grid of 1000×1000 equidistant points, ensuring a comprehensive coverage of the parameter plane. Figure 4(a) is drawn by coloring each point of the grid according to the period of the attractors. The colorbar, positioned on the right side of the figure, provides the periods of the attractors related to each color. To determine the period of a periodic attractor, we conduct an extensive time series analysis of the system. We first extract the time series data after removing the initial transients at each grid point and then analyze it to identify any repetitive patterns of the solution trajectory. An attractor is considered to have period s if the system revisits the same state after s number of steps.

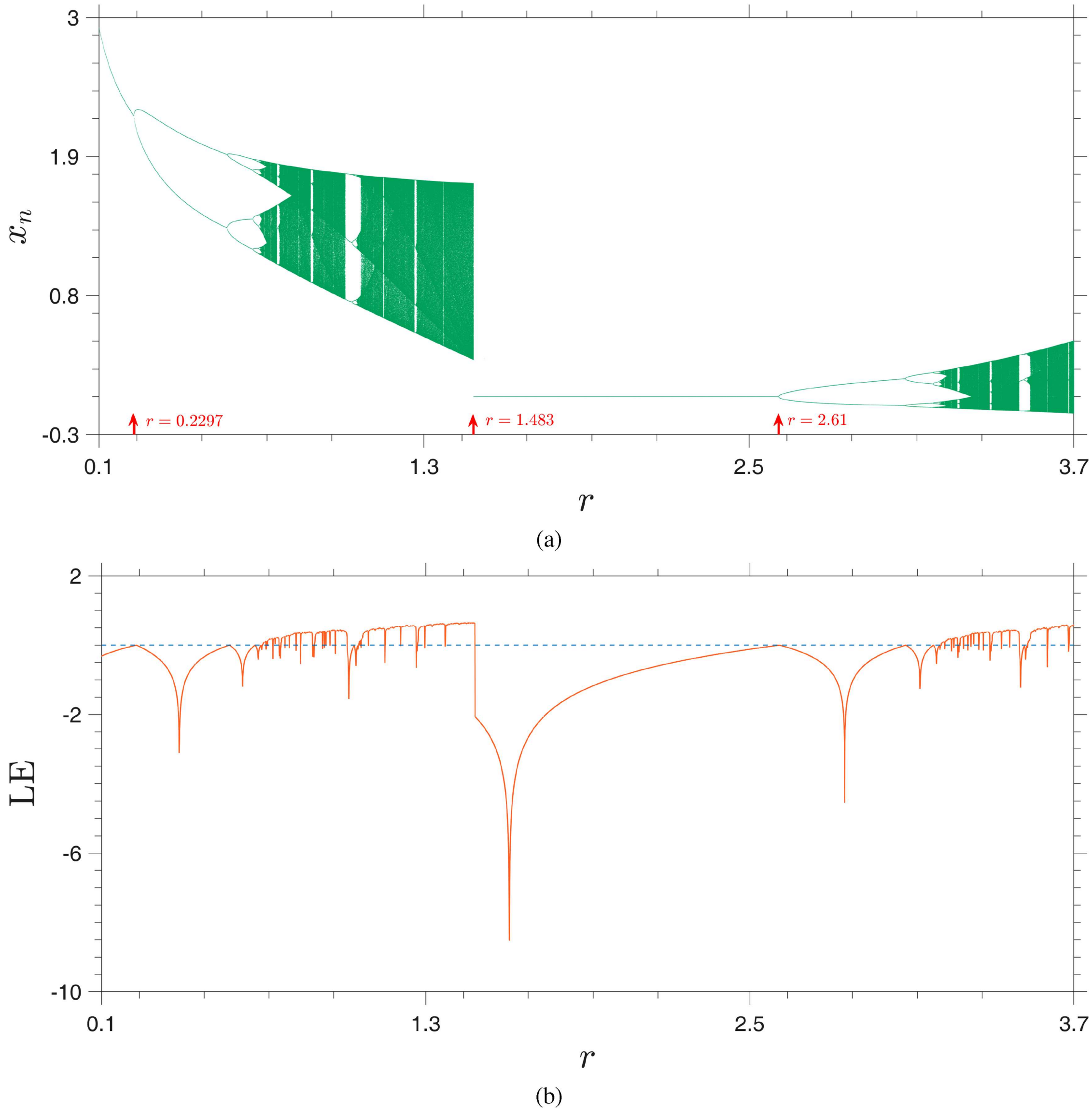

FIG. 2. (a) Bifurcation and (b) LE diagrams of system (5) for the variation of the control parameter r. As the parameter r increases, the system gradually becomes chaotic from stable state via period-doubling route around E_1. At $r = 1.483$, the system switches to a stable state (at E_0), and then after a sequence of period-doubling bifurcations, it again becomes chaotic around E_0. Within the chaotic zones (around E_0 and E_1), several periodic windows with different periodicity are apparent. Here, $\alpha = -0.61$ and values of k and A are fixed at 1 and 0.7, respectively.

In Fig. 4(a), attractors ranging from more than 17 period to 100 period are colored in white, while attractors exceeding 100 period are in black. Here, "FP_0" stands for trivial attractor (marked in pinkish red color), "FP" represents nonzero fixed point attractor (marked in deep green color), and "Unb." denotes the unbounded solutions (marked in light blue color). In Fig. 4(b), we calculate the values of Lyapunov exponent at each grid point and color each point according to the LE values given in the colorbar. The system's behavior is periodic or stable in the continuously changing white to orange-colored region (LE < 0). The rust color corresponds to bifurcation points (LE $= 0$). In the green to cyan-shaded region (LE > 0), the system exhibits chaotic oscillations. The blank region is related to unbounded solutions. Both the figures unveil complex and highly interleaved regions in the parameter plane, revealing a multitude of dynamical features. The shrimp-shaped periodic structures that emerge amidst the chaotic sea are of particular interest. Inside these

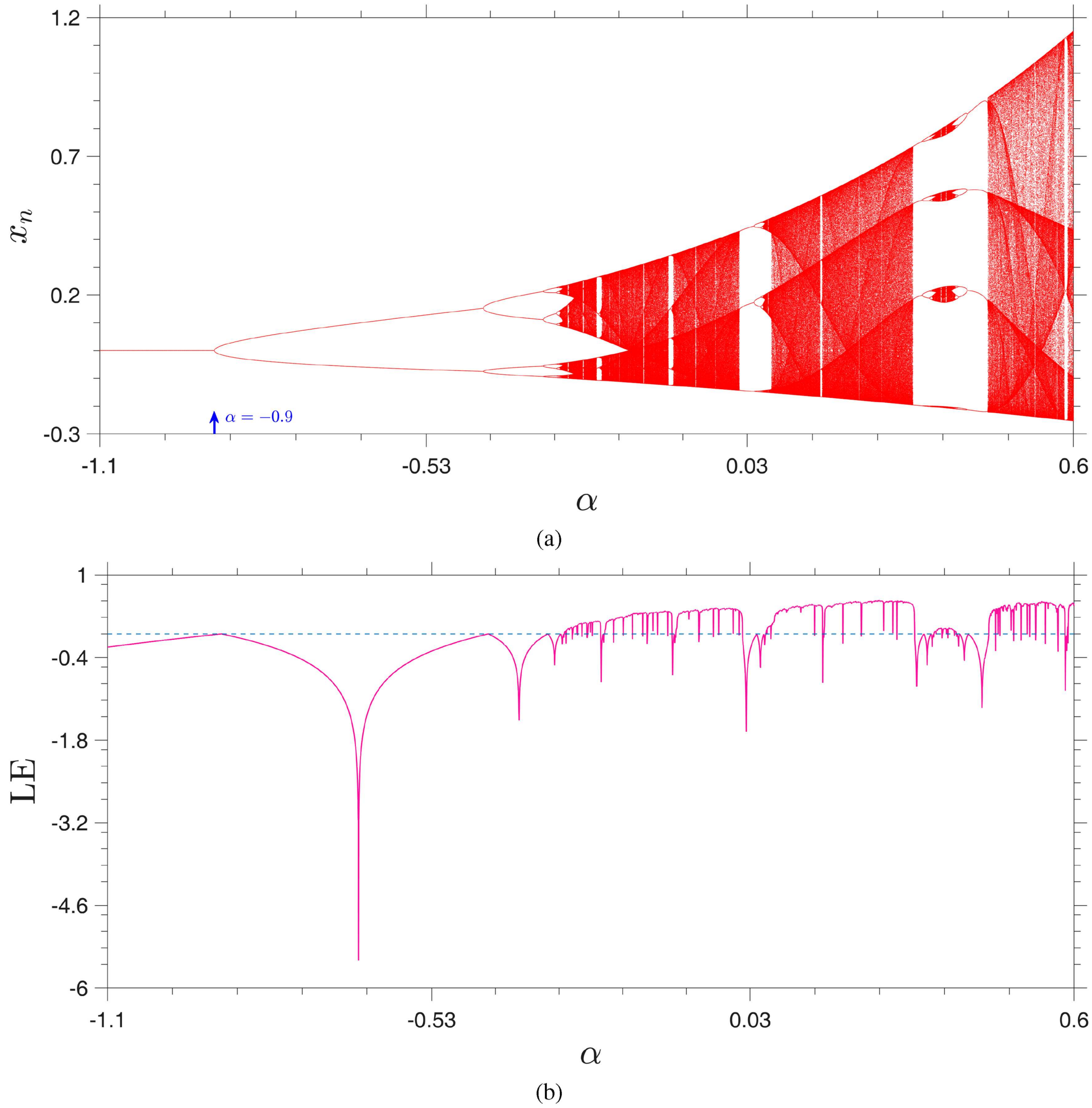

FIG. 3. (a) Bifurcation and (b) LE diagrams of system (5) for the variation of the control parameter α. As the parameter α increases, the system becomes chaotic from stable state via period-doubling route. Here, $r = 2.9$, and values of k and A are fixed at 1 and 0.7, respectively.

shrimp-shaped structures, there exist superstable cycles characterized by remarkably high stability. Some of these superstable cycles can be readily identified in Fig. 4(b), represented by white curves (LE $<< 0$).

A. Shrimp-shaped structure and period-bubbling route to chaos

A shrimp-shaped structure is a typically organized periodic structure characterized by a prominent central body and four elongated, slender antennae. Throughout the 1980s, several researchers observed these shrimp-like structures in various systems, though they were not initially labeled as "shrimps."[28–31] Moreover, numerous follow-up studies have revealed the presence of shrimp-like periodic structures. These periodic structures have been referred to by several names, including "swallow,"[32] "crossroad area,"[33] "compound window,"[34] etc. The name "shrimp" to describe these periodic structures was given and popularized by Gallas.[5,35] Vitolo *et al.*[36] provided the following definition for shrimp: "*Shrimps are formed by a regular set of adjacent windows centered around the main pair of intersecting superstable parabolic arcs. A shrimp is a doubly infinite mosaic of stability domains*

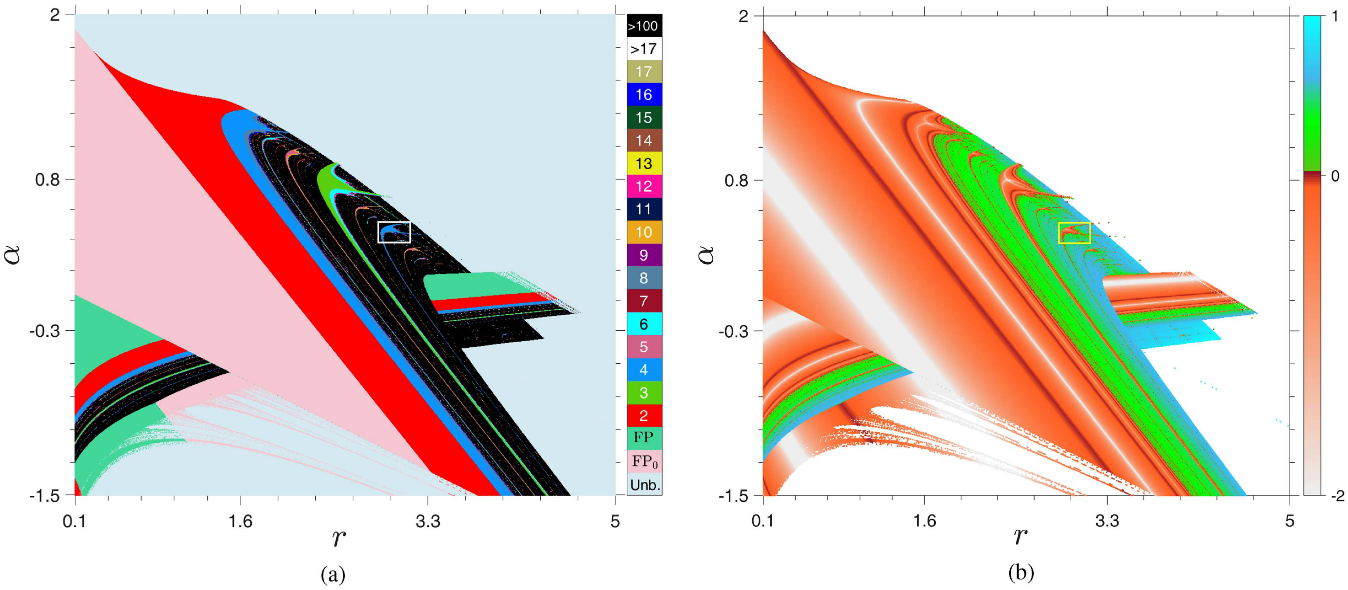

FIG. 4. Global view of the dynamics of the system represented by the (a) isoperiodic and (b) LE diagrams in the 1000 × 1000 grid points of $(r, \alpha) \in [0.1, 5] \times [-1.5, 2]$ parameter plane. Both diagrams reveal a multitude of dynamical features [stable state, periodicity (including higher-periodicity), chaos, etc.]. Notably, the presence of shrimp-shaped structures within the chaotic regime is clearly visible in both diagrams. The values of the parameters k and A are kept fixed at 1 and 0.7, respectively.

composed of an innermost main domain plus all the adjacent stability domains arising from two period-doubling cascades together with their corresponding domains of chaos." The presence of these complex shrimp-shaped periodic structures within chaotic regions is significant because it facilitates the control of chaos by selecting parameters within the shrimps. Recently, several researchers studied shrimp-shaped complex structures in parameter planes of many nonlinear systems.[37–39] In Figs. 4(a) and 4(b), we observe that the

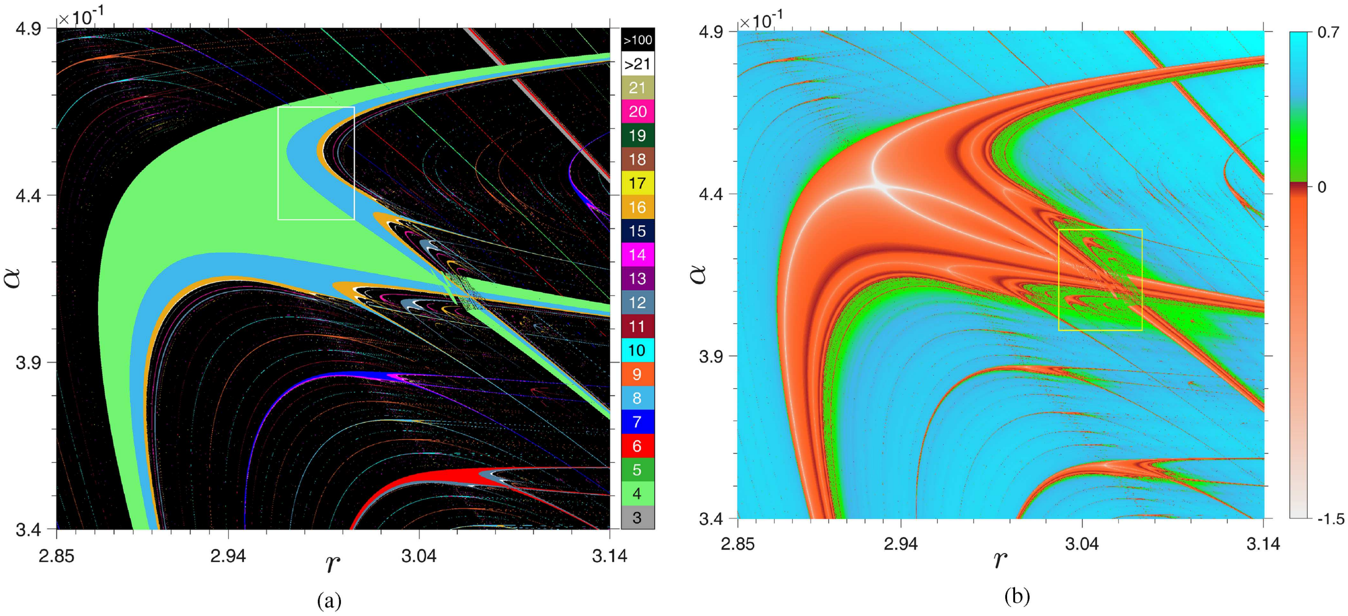

FIG. 5. Magnification of the regions enclosed by white and yellow rectangular boxes in Figs. 4(a) and 4(b), respectively. A comprehensive view of the shrimp-shaped structure of period 4 can be visualized from both panels. The values of k and A are fixed at 1 and 0.7, respectively.

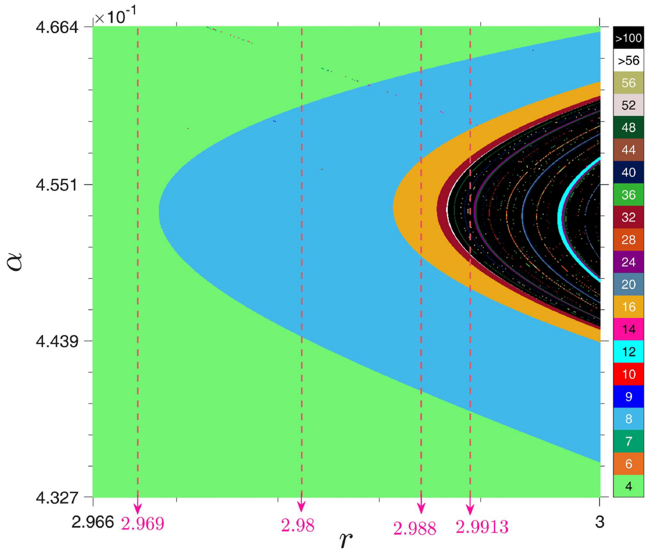

FIG. 6. Zoomed-in view of the region enclosed by the white rectangular box inside Fig. 5(a). It demonstrates that the system exhibits a period-bubbling phenomenon with respect to the variation of the parameter α. Here, $k = 1$ and $A = 0.7$.

chaotic regime is densely populated with numerous shrimp-shaped periodic structures. To thoroughly capture a complete understanding of one of those shrimp-shaped structures, we take fine-scale magnifications of the white and yellow rectangular boxes inside these figures [Figs. 4(a) and 4(b), respectively] and plot them in Figs. 5(a) and 5(b), respectively. These magnifications give a complete view of the shrimp-shaped structure of period 4. We see that two arrays of shrimp-shaped structures appear along the inner boundary of this shrimp-shaped structure, and they are organized almost in lines and the point of intersection of the superstable curves of each shrimp-shaped structure lies on these lines. In Fig. 5(a), saddle-node bifurcation creates the boundary between the black and light green regions. The boundaries between the light green and crystal blue regions, as well as the boundary separating the crystal blue and yellow-shaded regions, are due to period-doubling bifurcations. This pattern continues for the adjacent boundaries as well. In this way, a two-dimensional Feigenbaum scenario,[40] the path to chaos via a series of period-doubling bifurcations, is formed near the inner boundary of the shrimp-shaped structure. This is more obvious from Fig. 6, a zoomed-in view of the region enclosed by the white rectangular box in Fig. 5(a). In fact, in close proximity to the inner boundary of the shrimp-shaped structure, we observe the well-known period-bubbling[39] phenomenon. We will now explore this phenomenon in detail.

The concept of period-bubbling manifests as a notable phenomenon within the realm of nonlinear systems when a specific parameter of the system undergoes gradual and systematic variations. A sequence of events unfolds within this dynamic process: periodic attractors are generated through period-doubling bifurcations and subsequently disappear through reverse period-doubling bifurcations. This intricate sequence of bifurcations culminates in the formation of an intriguing bubble-shaped structure. To grasp the detail of the period-bubbling phenomenon, particularly near the inner boundary of a shrimp-shaped structure given in Fig. 5(a), we take an amplification of the inner region of the white box delineated within it. Figure 6 is the corresponding amplified diagram, illustrating the period-bubbling path to chaos. Here, the parameter α generates the period-bubbling path to chaos and r adjusts the breadth of the bubbles. Now, changing the value of α, while keeping the value of r constant at some discrete values, we discover that depending on the values of r, the system may or may not show the period-bubbling phenomenon. To confirm it, we draw four bifurcation diagrams in Fig. 7 along the four rust-dotted lines of Fig. 6 (from left to right). Figure 7(a) shows four curves at $r = 2.969$ with respect to change of the parameter α, where no bubble is formed. Figure 7(b) presents the period 4×2 bubble at $r = 2.98$. In Fig. 7(c) ($r = 2.988$), a period 4×4 bubble is formed inside the original period 4×2 bubble. As r increases, smaller and smaller bubbles are formed within these larger bubbles, leading to the creation of a continuously branching tree of bubbles. This ultimately leads to the emergence of chaos, as depicted in Fig. 7(d) ($r = 2.9913$). For a finer visualization of this bubble formation process, see the animation "Anim_bubbling.mp4" in the supplementary material.

The literature on shrimp-shaped structures has established a captivating universal feature: three times self-similarity.[41] This characteristic of the shrimp-shaped structures can be demonstrated in system (5) through fine-scale magnifications. Figure 8(a) is the magnification of the interior area of the yellow-colored box inside Fig. 5(b). In this figure, we observe that two smaller shrimps with higher periodicity appear close to the inner legs of the shrimp-shaped structure of period 4. The periodicities of these two shrimps are 12, three times of the periodicity of the bigger shrimp. To further explore this pattern, we amplify the yellow-colored rectangular area in Fig. 8(a), which is located near the inner leg of the shrimp of period 12. The zoomed-in view, as shown in Fig. 8(b), reveals a similar feature. By applying subsequent amplifications with appropriate scaling, we observe a repetition of these small shrimp-shaped structures and see that the periodicities of these small shrimps are always three times that of the associated larger shrimp, namely, 36, 108, 324, and so on. Hence, shrimp-shaped structures, their three times self-similar properties and period-bubbling route to chaos can be found in this rather simple one-dimensional model.

B. Bistability between different attractors

Multistability is a fascinating phenomenon with potential applications in a variety of fields.[20,42–45] It refers to a phenomenon in which a system can exhibit multiple states purely through the manipulation of initial conditions without invoking any adjustments in the underlying parameters of the system. Specifically, when a system has precisely two such states, this phenomenon is termed as bistability. In essence, bistability exemplifies a subset of the broader multistability phenomenon, where two distinct attractors coexist, thereby enhancing the complexity and richness of the system's dynamics.

In Fig. 8(a), we observe overlappings between several pairs of coexisting attractors, which indicates the presence of bistability between different attractors in system (5). To confirm such

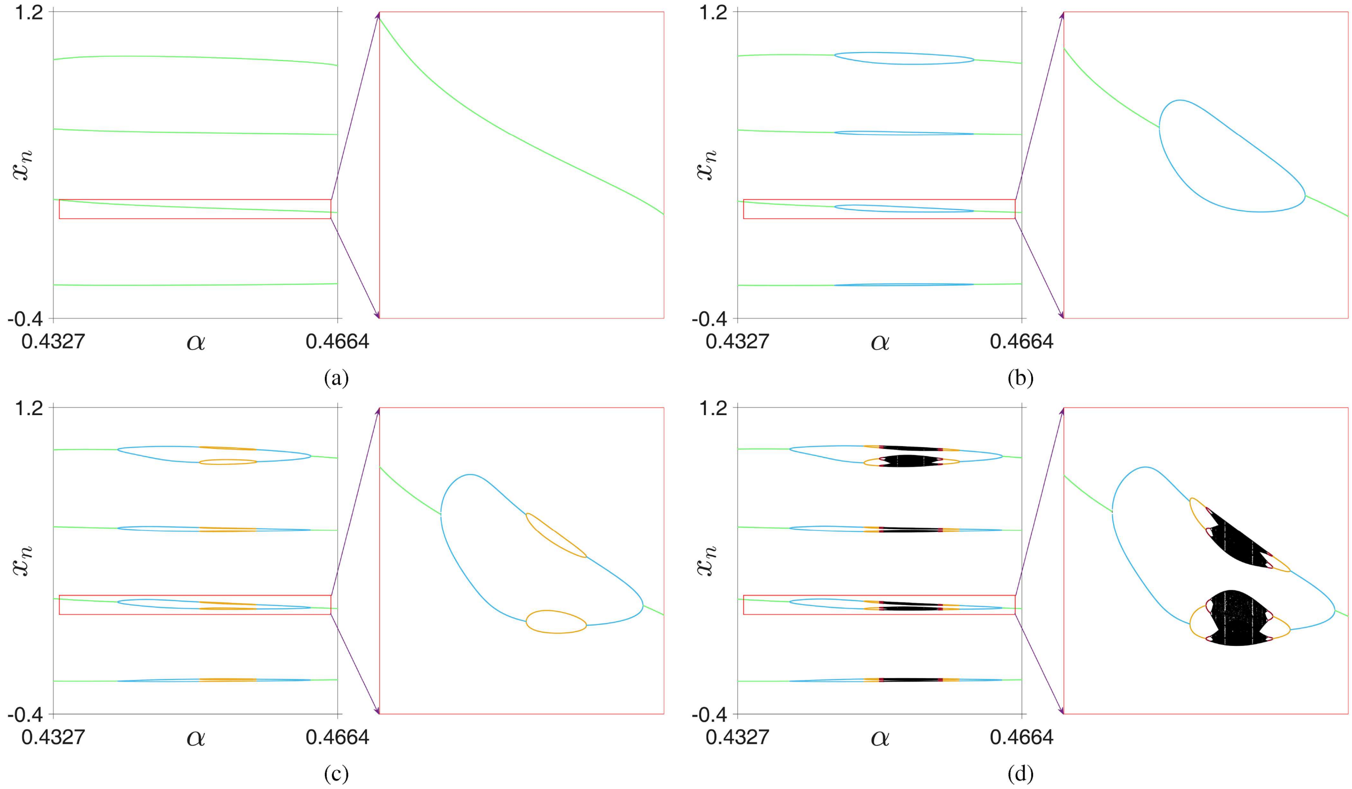

FIG. 7. Bifurcation diagrams along the four dotted lines in Fig. 6, demonstrating the emergence of chaos through period-bubbling path near the inner edge of the shrimp-shaped structure. Here, $k = 1$, $A = 0.7$, and for (a) $r = 2.969$, for (b) $r = 2.98$, for (c) $r = 2.988$, and, finally, for (d) $r = 2.9913$.

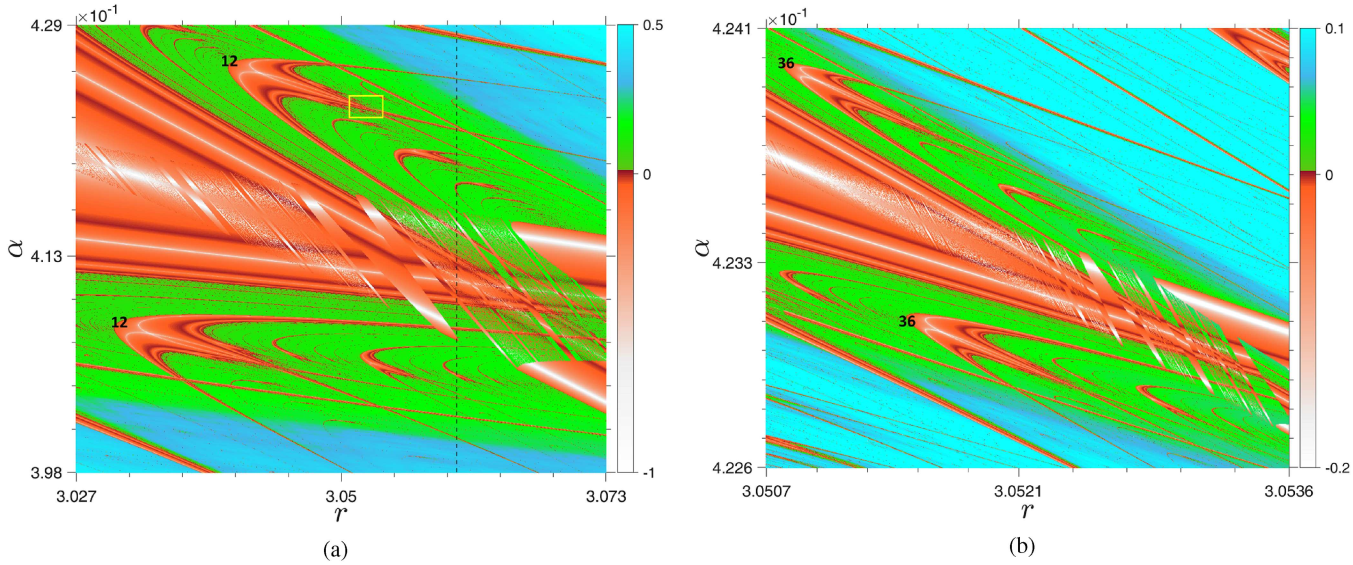

FIG. 8. (a) Enlargement of the region bounded by the yellow-colored rectangular box of Fig. 5(b). (b) Magnification of the interior area of the yellow-colored box inside (a). Both diagrams show the three times self-similarity of the shrimp-shaped structure. The numbers at the top of the shrimps represent their respective periodicities.

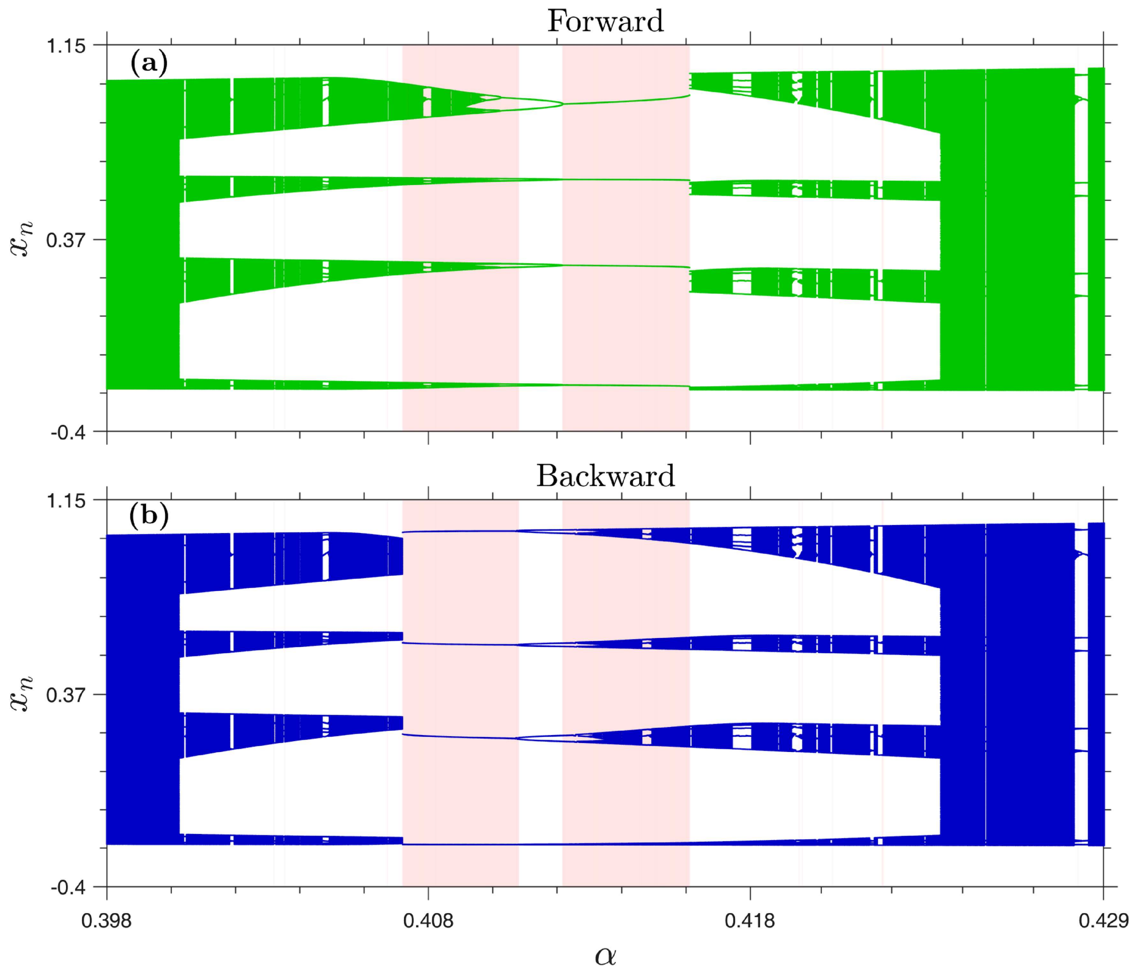

FIG. 9. Bifurcation diagrams for two different methods of "following the attractor," (a) forward and (b) backward, displaying bistability between different pairs of attractors (highlighted by light pink-colored rectangular filled boxes). The starting initial condition for each diagram is $x_0 = 0.3$. The values of r, k, and A are fixed at 3.06, 1, and 0.7, respectively.

an indication, we draw two bifurcation diagrams in Fig. 9 using the conventional approach of "following the attractor" (the way of changing initial states): forward and backward, along the black line ($r = 3.06$) in Fig. 8(a). In the attractor-following approach, we begin at one end of the parameter interval with a fixed initial condition. As we move to the next subsequent point in the interval, we no longer use the fixed initial condition. Instead, the final point from the previously computed solution is used as the new initial condition. We repeat this procedure until reaching the other end of the parameter interval, effectively following the attractor throughout the interval. It plays a fundamental role in identifying the parameter regions associated with multistability,[21,22] i.e., the presence of coexisting attractors in phase space. Based on the choice of starting point, we have two different types of bifurcation diagram by "following the attractor" method: forward and backward. If the forward and backward bifurcation diagrams do not appear identical or perfectly overlap, it indicates the presence of multistability. The parameter intervals, where the diagrams differ, represent the multistable zones. In Fig. 9, the diagram with green dots is the forward bifurcation diagram (for increasing values of α), and the one with navy blue dots is the backward bifurcation diagram (for decreasing values of α). Both diagrams are generated by running the simulations in the following manner: for the smallest (or largest) value of $\alpha \in [0.398, 0.429]$, the initial state is set to $x_0 = 0.3$; for each subsequent value of α, the last point of the previously determined solution, i.e., solution derived for earlier value of α serves as the initial state and we repeat this procedure until we reach $\alpha = 0.429$ (or $\alpha = 0.398$). Both the forward and backward bifurcation diagrams look identical except for specific parameter intervals (highlighted by light pink-colored rectangular filled boxes), within which system (5) exhibits bistable behavior. By closely inspecting these two diagrams, we identify bistability between multiple pairings

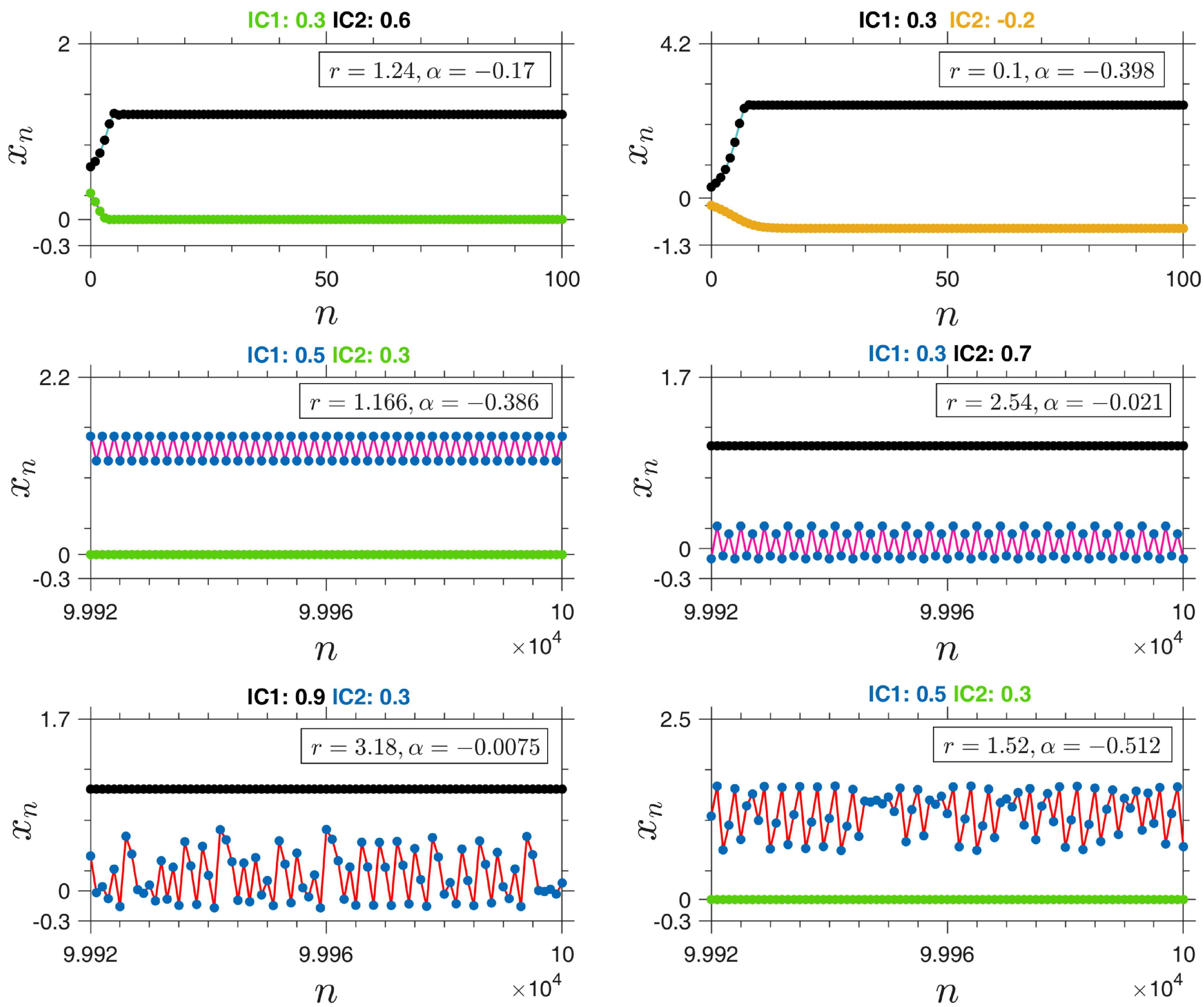

FIG. 10. Time series plots corresponding to the six different bistable phenomena within the $r-\alpha$ parameter plane. Here, $k = 1$, $A = 0.7$, and the other parameter values are given in the upper-right corner of each time series plot. Also, the corresponding initial conditions are provided in the title of each plot.

of attractors (periodic–periodic and periodic–chaotic). The bistability between period 4 and the chaotic attractor is the most significant one. It appears prominently in two distinct zones of Fig. 9. These bistable zones are exciting in the context of predictability of the dynamics of the system in the long run as a small change in the initial state might cause the system to switch from periodic to chaotic oscillations or vice versa.

Furthermore, close inspections of Figs. 1 and 4 reveal that system (5) manifests a multitude of distinct bistable phenomena beyond the previously observed bistability involving periodic and chaotic attractors or bistability between periodic and periodic attractors. For example, bistability between E_0 stable–E_1 stable, E_1 stable–E_2 stable, periodicity 2 (around E_1)–E_0 stable, periodicity 4 (around E_0)–E_1 stable, chaos (around E_0)–E_1 stable, chaos (around E_1)–E_0 stable, and many others can be found. To verify the presence of these types of bistability in system (5), we plot time series solutions for different initial conditions corresponding to the bistable points in the $r-\alpha$ parameter plane (see Fig. 10). Through this analysis, we observe that the system converges to distinct attractors for different sets of initial conditions.

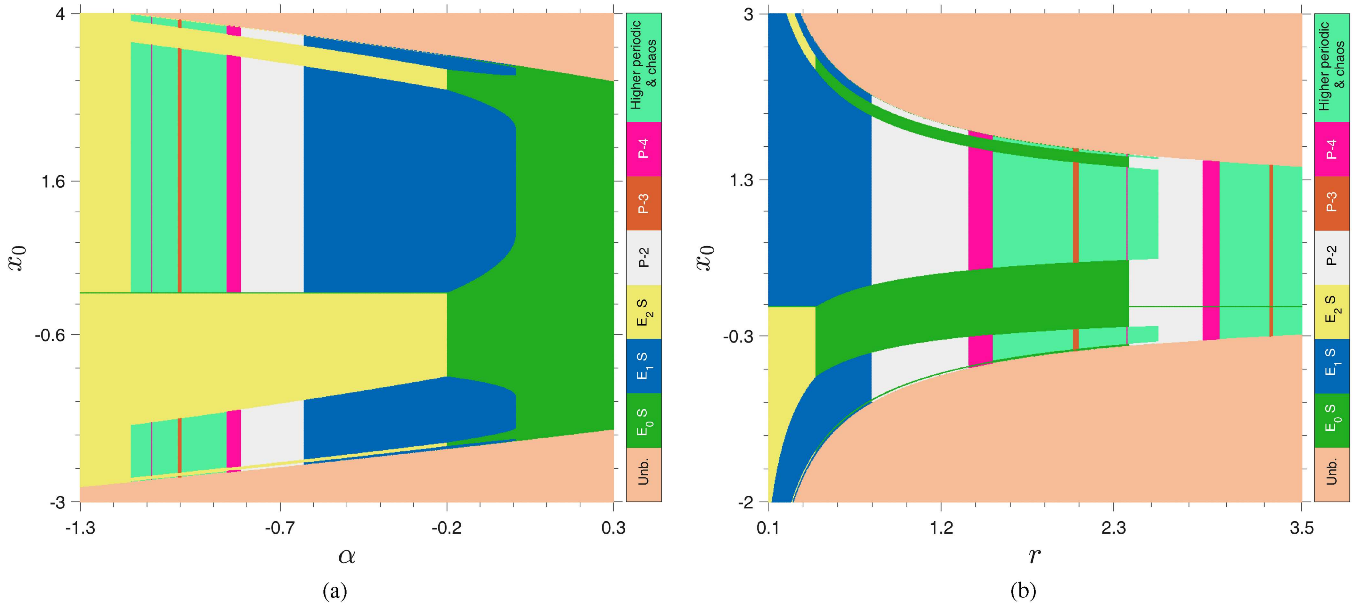

FIG. 11. Emergence of different attractors for the simultaneous changes in (a) α and x_0, while r is fixed at 0.2, and (b) r and x_0, while α is fixed at -0.4. The values of k and A are kept fixed at 1 and 0.7, respectively. Colorbars represent the characteristics of the attractors according to the respective colors.

From Fig. 10, it becomes apparent that the system converges to different attractors for various combinations of r and α values, as well as for different initial conditions (x_0). To visualize the transition of these attractors, we construct two diagrams in Fig. 11. The first one is plotted in the $\alpha - x_0$ plane for $r = 0.2$ [Fig. 11(a)] and the other one in the $r - x_0$ plane for $\alpha = -0.4$ [Fig. 11(b)]. Both diagrams vividly illustrate that the system's behavior undergoes transitions between various attractors, namely E_0 stable (E_0S), E_1 stable (E_1S), E_2 stable (E_2S), period 2 (P-2), period 3 (P-3), period 4 (P-4), and higher periodic and chaotic attractors depending on the specific values of α or r, and the chosen initial conditions. It is essential to highlight that the reddish orange regions within the diagrams, labeled as "Unb.," signify sets of (α, x_0) or (r, x_0) values for which system (5) has unbounded solutions.

Now, we give the following remarks:

Remark III.1. *We observe that system (5) exhibits distinct zones of "chaos and non-chaos" behaviors in the $k - A$ parameter plane also. Figure 12 provides a global view of the isoperiodic diagram in the $(k, A) \in [0.4, 2] \times [0.4, 2]$ parameter plane, which is generated by setting $r = 2.5$ and $\alpha = 0.8$. We find that the organization of the periodic and chaotic zones is different from those observed in the $(r, \alpha) \in [0.1, 5] \times [-1.5, 2]$ parameter plane. Additionally, no shrimp-shaped periodic structures appear within the chaotic regime, although periodic bands of various periods are clearly visible. It is important to note that we have excluded the investigation of the system dynamics in the light violet-colored region of the parameter plane as this region ($A > k$) is not feasible in the context of modeling assumptions. To further visualize the individual effects of the parameters k and A on the dynamics of the system within the same $(r, \alpha) \in [0.1, 5] \times [-1.5, 2]$ parameter plane, we have added two animated movies, "Anim_lyap_k.mp4" and "Anim_lyap_A.mp4," in the supplementary material. These animations demonstrate that the system exhibits similar types of dynamical*

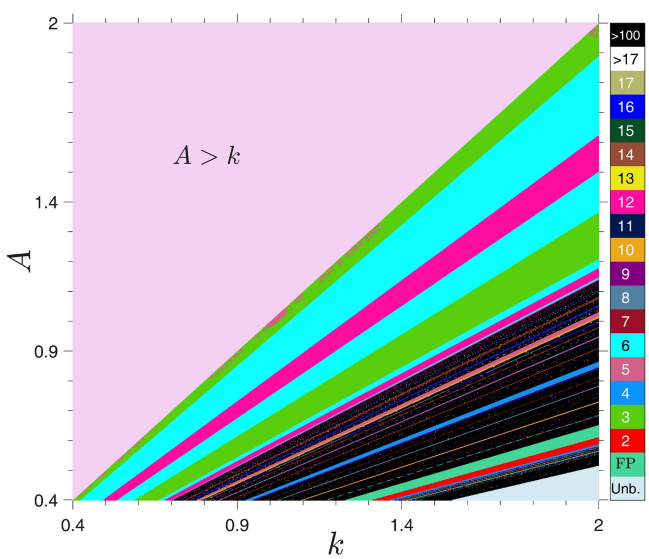

FIG. 12. Isoperiodic diagram of the system in the $k - A$ parameter plane ($(k, A) \in [0.4, 2] \times [0.4, 2]$), illustrating the diverse dynamical features of system (5) within this parameter plane. The light violet-colored region ($A > k$) is not feasible in the context of the model (5). Here, $r = 2.5$ and $\alpha = 0.8$.

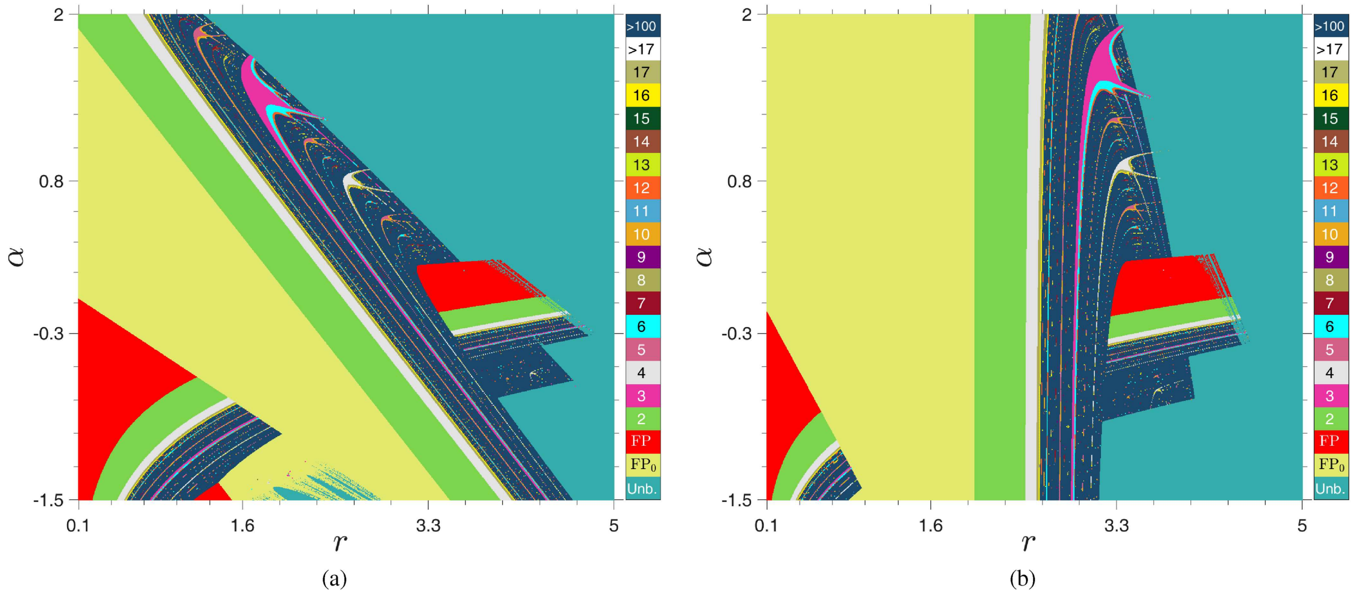

FIG. 13. Different dynamical scenarios for (a) $f(x) = \dfrac{\alpha x}{1+x}$ and (b) $f(x) = \dfrac{\alpha x^2}{1+x^2}$. The values of the parameters k and A are kept fixed at 1 and 0.7, respectively.

behaviors for the individual variations of k and A within this parameter plane. The changes in these two parameters mainly shift the specific positions of the regions where different dynamical scenarios occur.

Remark III.2. *Instead of assuming a fixed proportion of capital outflow or inflow ($f(x) = \alpha x$), if we consider two different functional forms (saturating type) to model the outflow or inflow of capital: $f(x) = \dfrac{\alpha x}{1+x}$ and $f(x) = \dfrac{\alpha x^2}{1+x^2}$ when conducting numerical simulations using the same parameter values and initial condition, we observe similar behavioral patterns as depicted in Fig. 4(a). In this context, Fig. 13(a) represents the isoperiodic diagram for $f(x) = \dfrac{\alpha x}{1+x}$, while Fig. 13(b) corresponds to $f(x) = \dfrac{\alpha x^2}{1+x^2}$ in the $(r, \alpha) \in [0.1, 5] \times [-1.5, 2]$ parameter plane. The key difference is the positioning of areas representing diverse dynamical behaviors. Therefore, although the overall behavioral patterns are akin, the precise positions within the parameter plane, where these behaviors manifest, differ for these three forms of f(x).*

Remark III.3. *Here, it is worth mentioning that system (4) with $f(x) = \alpha x$ [i.e., the continuous-time counterpart of system (5)] has the same set of equilibrium points existing under the same parametric constraints as system (5). The transcritical and saddle-node bifurcation curves of the continuous system in the $r - \alpha$ parameter plane are identical to the curves drawn in the same parameter plane for system (5). However, unlike system (5), which can undergo period-doubling/period-halving bifurcation leading to more complex dynamical behavior, we find that its continuous-time counterpart does not exhibit a period-doubling/period-halving bifurcation.*

IV. CONCLUSION

In the present study, we have formulated a one-dimensional discrete-time economic model and explored its intrinsic dynamical features analytically and numerically. We have studied the individual impact of two vital system parameters on the system's transition through various dynamical states, including stable state, periodicity, and chaos. The emergence of chaos makes predicting the behavior of a system extremely difficult and even impossible in the long-term. A chaotic economic system challenges economists to explore economic phenomena on a deeper level. Moving a step further, we have explored the system's dynamics in the parameter plane formed by the simultaneous variation of two control parameters. We have observed periodic shrimp-shaped structures within the chaotic regime of the parameter plane and discussed some of their universal properties. The appearance of such periodic structures within the chaotic regime gives an idea about how to attain favorable economic scenarios (i.e., periodic or predictable patterns) by eliminating unfavorable ones (i.e., chaotic or unpredictable patterns) through an appropriate adjustment of the parameter values across the wide areas of these periodic structures. Another intriguing phenomenon observed in the system is the occurrence of bistability between different sets of attractors. A bistable system always exhibits path dependence, which means that its long-term behavior is strongly influenced by the initial condition, so even a small perturbation in the initial condition can significantly impact its behavior. From an economic perspective, it signifies how different economic situations, like higher incomes, preventing a company's bankruptcy or improving the economy, etc., can be achieved by altering the initial values of the economic components of that economic system. In particular, the presence of bistability in the context of capital signifies that the company's capital can hop between two states depending on the initial amount of capital in the company. This has important implications for decision-making, risk management, and strategic planning. Therefore, understanding the initial conditions those lead to transitions between more profitable states can offer valuable insights into the company's financial resilience and vulnerability. In summary, the present study illustrates the importance of variations in vital system parameters and the selection of an initial amount of capital, which may assist economists in predicting prospective changes in the financial landscape and making decisions to navigate pitfalls effectively.

SUPPLEMENTARY MATERIAL

See the supplementary material for the following:

Anim_bif_r.mp4: The animation shows the evolution of the attractors along the bifurcation diagram shown in Fig. 2(a). It provides a clear insight into the alterations in the system's dynamics due to variations of the parameter r.

Anim_bif_alpha.mp4: The animation demonstrates the unfolding of the attractors along the bifurcation diagram given in Fig. 3(a). It offers a more vivid insight into how variations in the parameter α bring changes in the dynamics of the system.

Anim_bubbling.mp4: The animation shows the period-bubbling phenomenon along the inner boundary of the shrimp-shaped structure given in Fig. 5(a). To be more specific, it showcases the emergence of the period-bubbling phenomenon as the parameter r is increased, as demonstrated on the isoperiodic diagram presented in Fig. 6. Additionally, it provides a clear visualization of how the parameter α leads to the creation of a path from period-bubbling to chaotic behavior, while the parameter r modulates the width of these bubbles.

Anim_lyap_k.mp4: The animation illustrates the impact of the parameter k on the system's dynamics within the $(r, \alpha) \in [0.1, 5] \times [-1.5, 2]$ parameter plane. It specifically demonstrates how the Lyapunov exponent diagram evolves in this parameter plane as k varies within the range $[0.75, 4]$.

Anim_lyap_A.mp4: The animation shows how the parameter A affects the dynamics of the system in the $(r, \alpha) \in [0.1, 5] \times [-1.5, 2]$ parameter plane. It highlights the changes in the Lyapunov exponent diagram when A varies in the interval $[0.1, 0.98]$.

ACKNOWLEDGMENTS

We are thankful to the honorable Editor and the anonymous reviewers for their valuable comments and suggestions that improved the quality of the manuscript. Ruma Kumbhakar is thankful to the UGC, India, for providing financial support under the Senior Research Fellowship program (NTA Ref. No. 191620068570). Sarbari Karmakar is grateful to the CSIR, India, for providing financial support under the Senior Research Fellowship program (File No. 09/0202(13708)/2022-EMR-I).

AUTHOR DECLARATIONS

Conflict of Interest

The authors have no conflicts to disclose.

Author Contributions

Ruma Kumbhakar: Conceptualization (equal); Investigation (equal); Methodology (equal); Software (equal); Validation (equal); Visualization (equal); Writing – original draft (equal); Writing – review & editing (equal). **Sarbari Karmakar:** Conceptualization (equal); Formal analysis (equal); Investigation (equal); Validation (equal); Visualization (equal); Writing – original draft (equal); Writing – review & editing (equal). **Nikhil Pal:** Conceptualization (equal); Resources (equal); Supervision (equal); Validation (equal); Visualization (equal); Writing – original draft (equal); Writing – review & editing (equal). **Jürgen Kurths:** Conceptualization (equal); Resources (equal); Supervision (equal); Validation (equal); Visualization (equal); Writing – original draft (equal); Writing – review & editing (equal).

DATA AVAILABILITY

The data (set of parameters) that support the findings of this study are available within the article.

REFERENCES

[1] W.-B. Zhang, *Discrete Dynamical Systems, Bifurcations and Chaos in Economics* (Elsevier, New York, 2006).
[2] R. M. May, "Biological populations with nonoverlapping generations: Stable points, stable cycles, and chaos," Science **186**, 645–647 (1974).
[3] M. J. Stutzer, "Chaotic dynamics and bifurcation in a macro model," J. Econ. Dyn. Control **2**, 353–376 (1980).
[4] M. Guzowska and E. Michetti, "Local and global dynamics of Ramsey model: From continuous to discrete time," Chaos **28**, 055902 (2018).
[5] J. A. C. Gallas, "Dissecting shrimps: Results for some one-dimensional physical models," Phys. A **202**, 196–223 (1994).
[6] R. M. May, "Simple mathematical models with very complicated dynamics," Nature **261**, 459–467 (1976).
[7] T. Puu and I. Sushko, "A business cycle model with cubic nonlinearity," Chaos, Solitons Fractals **19**, 597–612 (2004).
[8] D. F. M. Oliveira and E. D. Leonel, "Parameter space for a dissipative Fermi–Ulam model," New J. Phys. **13**, 123012 (2011).
[9] J. R. Beddington, C. A. Free, and J. H. Lawton, "Dynamic complexity in predator-prey models framed in difference equations," Nature **255**, 58–60 (1975).
[10] R. Dieci, G. I. Bischi, and L. Gardini, "From bi-stability to chaotic oscillations in a macroeconomic model," Chaos, Solitons Fractals **12**, 805–822 (2001).
[11] B. LeBaron, "Chaos and nonlinear forecastability in economics and finance," Philos. Trans. R. Soc. London, A **348**, 397–404 (1994).
[12] L. Gardini, L. Gori, L. Guerrini, and M. Sodini, "Introduction to the focus issue 'nonlinear economic dynamics'," Chaos **28**, 055801 (2018).
[13] T. Puu, "Chaos in business cycles," Chaos, Solitons Fractals **1**, 457–473 (1991).
[14] G. I. Bischi, L. Gardini, and M. Kopel, "Analysis of global bifurcations in a market share attraction model," J. Econ. Dyn. Control **24**, 855–879 (2000).
[15] M. T. Pohjola, "Stable, cyclic and chaotic growth: The dynamics of a discrete-time version of Goodwin's growth cycle model," J. Econ. **41**, 27–38 (1981), https://www.jstor.org/stable/41798053
[16] R. M. Goodwin, "A growth cycle," in *Socialism, Capitalism and Economic Growth*, edited by C. H. Fenstein (Cambridge University Press, Cambridge, 1967).
[17] R. H. Day, "Irregular growth cycles," Am. Econ. Rev. **72**, 406–414 (1982), https://www.jstor.org/stable/1831540
[18] R. M. Solow, "A contribution to the theory of economic growth," Q. J. Econ. **70**, 65–94 (1956).
[19] G. I. Bischi and F. Tramontana, "Three-dimensional discrete-time Lotka–Volterra models with an application to industrial clusters," Commun. Nonlinear Sci. Numer. Simul. **15**, 3000–3014 (2010).
[20] A. N. Pisarchik and U. Feudel, "Control of multistability," Phys. Rep. **540**, 167–218 (2014).

[21] C. Manchein, L. Santana, R. M. da Silva, and M. W. Beims, "Noise-induced stabilization of the Fitzhugh–Nagumo neuron dynamics: Multistability and transient chaos," Chaos **32**, 083102 (2022).
[22] C. Manchein, B. Fusinato, H. S. Chagas, and H. A. Albuquerque, "Quint points lattice and multistability in a damped-driven curved carbon nanotube oscillator model," Chaos **33**, 063147 (2023).
[23] A. Agliari, A. K. Naimzada, and N. Pecora, "Nonlinear dynamics of a Cournot duopoly game with differentiated products," Appl. Math. Comput. **281**, 1–15 (2016).
[24] A. Panchuk, I. Sushko, and F. Westerhoff, "A financial market model with two discontinuities: Bifurcation structures in the chaotic domain," Chaos **28**, 055908 (2018).
[25] N. C. Pati, S. Garai, M. Hossain, G. C. Layek, and N. Pal, "Fear induced multistability in a predator-prey model," Int. J. Bifurc. Chaos **31**, 2150150 (2021).
[26] M. Hossain, R. Kumbhakar, N. Pal, and J. Kurths, "Structure of parameter space of a three-species food chain model with immigration and emigration," Nonlinear Dyn. **111**, 14565–14582 (2023).
[27] S. Garai, M. Hossain, S. Karmakar, and N. Pal, "Chaos, periodic structures, and multistability: Complex dynamical behaviors of an eco-epidemiological model in parameter planes," Chaos **33**, 083115 (2023).
[28] H. El Hamouly and C. Mira, "Lien entre les propriétés d'un endomorphisme de dimension un et celles d'un difféomorphisme de dimension deux," C. R. Acad. Sci. Paris Sér. I Math **293**, 525–528 (1981).
[29] S. Fraser and R. Kapral, "Analysis of flow hysteresis by a one-dimensional map," Phys. Rev. A **25**, 3223–3233 (1982).
[30] L. Glass, M. R. Guevara, J. Belair, and A. Shrier, "Global bifurcations of a periodically forced biological oscillator," Phys. Rev. A **29**, 1348–1357 (1984).
[31] R. S. Mackay and C. Tresser, "Some flesh on the skeleton: The bifurcation structure of bimodal maps," Phys. D **27**, 412–422 (1987).
[32] J. Milnor, "Remarks on iterated cubic maps," Exp. Math. **1**, 5–24 (1992), https://www.tandfonline.com/doi/abs/10.1080/10586458.1992.10504242
[33] J. P. Carcasses, C. Mira, M. Bosch, C. Simó, and J. C. Tatjer, "'Crossroad area–spring area' transition (I) parameter plane representation," Int. J. Bifurc. Chaos **01**, 183–196 (1991).
[34] E. N. Lorenz, "Compound windows of the Hénon-map," Phys. D **237**, 1689–1704 (2008).
[35] J. A. C. Gallas, "Structure of the parameter space of the Hénon map," Phys. Rev. Lett. **70**, 2714 (1993).
[36] R. Vitolo, P. Glendinning, and J. A. C. Gallas, "Global structure of periodicity hubs in Lyapunov phase diagrams of dissipative flows," Phys. Rev. E **84**, 016216 (2011).
[37] Y. Zou, M. Thiel, M. C. Romano, J. Kurths, and Q. Bi, "Shrimp structure and associated dynamics in parametrically excited oscillators," Int. J. Bifurc. Chaos **16**, 3567–3579 (2006).
[38] R. Kumbhakar, M. Hossain, and N. Pal, "Dynamics of a two-prey one-predator model with fear and group defense: A study in parameter planes," Chaos, Solitons Fractals **179**, 114449 (2024).
[39] M. Hossain, S. Garai, S. Jafari, and N. Pal, "Bifurcation, chaos, multistability, and organized structures in a predator–prey model with vigilance," Chaos **32**, 063139 (2022).
[40] M. J. Feigenbaum, "Universal behavior in nonlinear systems," Phys. D **7**, 16–39 (1983).
[41] S. L. T. de Souza, A. A. Lima, I. L. Caldas, R. O. Medrano-T, and Z. D. O. Guimarães-Filho, "Self-similarities of periodic structures for a discrete model of a two-gene system," Phys. Lett. A **376**, 1290–1294 (2012).
[42] A. Akgul, O. F. Boyraz, K. Rajagopal, E. Guleryuz, M. Z. Yildiz, and M. Kutlu, "An unforced megastable chaotic oscillator and its application on protecting electrophysiological signals," Z. Naturforsch. A **75**, 1025–1037 (2020).
[43] G. Peng and F. Min, "Multistability analysis, circuit implementations and application in image encryption of a novel memristive chaotic circuit," Nonlinear Dyn. **90**, 1607–1625 (2017).
[44] S. Fang, S. Zhou, D. Yurchenko, T. Yang, and W.-H. Liao, "Multistability phenomenon in signal processing, energy harvesting, composite structures, and metamaterials: A review," Mech. Syst. Signal Process. **166**, 108419 (2022).
[45] H. Jahanshahi, K. Rajagopal, A. Akgul, N. N. Sari, H. Namazi, and S. Jafari, "Complete analysis and engineering applications of a megastable nonlinear oscillator," Int. J. Non-Linear Mech. **107**, 126–136 (2018).